

Direct Electrosynthesis of Polyaniline-Fe₂O₃ Nanocomposite Coating on Aluminum Alloy 5052 and Its Corrosion Protection Performance

M. Shabani-Nooshabadi*, S. M. Ghoreishi, H. Eghbali-Bidgoli, Y. Jafari

Department of Analytical Chemistry, Faculty of Chemistry, University of Kashan, Kashan, I.R. Iran.

Article history:

Received 25/09/2015

Accepted 11/11/2015

Published online 01/12/2015

Keywords:

Polyaniline- Fe₂O₃

Electrosynthesis

Aluminum alloy 5052

Corrosion

*Corresponding author:

E-mail address:

m.shabani@kashanu.ac.ir

Abstract

The synthesis of polyaniline- Fe₂O₃ nanocomposite coating on aluminum Alloy 5052 (AA5052) surface has been investigated by using the galvanostatic method. The anticorrosion performance of polyaniline-Fe₂O₃ coating was investigated in 3.5% NaCl solution by the open- circuit potential (OCP), Tafel polarization technique and Electrochemical Impedance Spectroscopy (EIS). The corrosion rate of polyaniline-Fe₂O₃ nanocomposite coating AA5052 was found about 140 times lower than bare AA5052. Corrosion potential also decreased from -0.710 V to -0.735 V versus Ag/AgCl for uncoated AA5052 and polyaniline-Fe₂O₃ nanocomposite coated on AA5052 electrodes, respectively. Electrochemical measurements show that polyaniline-Fe₂O₃ nanocomposite coated has good inhibitive properties with PE% of ~97.3% at 25 mA cm⁻² current density applied on AA5052 corrosion in a chloride media. The results of this study clearly find out that the polyaniline-Fe₂O₃ nanocomposite has an outstanding possible to protect AA5052 against corrosion in a chloride environment.

2015 JNS All rights reserved

1. Introduction

Aluminum alloys have applications in aerospace, transportation and beverage industries because of their lightweight and high strength properties [1]. Aluminum, a very reactive metal, forms a thin solid protecting film of oxide which prevents the further corrosion of the material. However, in contact with solutions containing complex agents (i.e. halides), aluminum undergoes localized corrosion various

attempts have been made to study the influence of different ions on the electrochemical behavior and pitting corrosion of Al and its alloys [2, 3].

Protecting aluminum by covering its surface with an organic coating is a good way for taking advantages of the mechanical property of the metal while protecting it from corrosion. Adhesion of these organic coatings on aluminum is very poor and needs some pretreatment like chromating. Due to the

carcinogenic nature of chromate conversion coatings, there is a high demand for an environmentally friendly surface treatment [4-9].

Conducting polymers such as polypyrrole (PPy), polyaniline (PANI) and their derivatives have been studied due to their electrical conductivity, reversible electrochemical behavior, electrical and optical properties and so forth. PANI is also a p-type semiconductor which can be synthesized by both electrochemical and chemical methods [10, 11].

Several applications of PANI have been known like in sensors [12, 13], batteries [14, 15], and as anti-corrosive additive inorganic coatings [16-18]. Many works indicated that PANI is a good candidate for anticorrosion coatings on metals in acid and saline media [19, 20]. The mechanism of corrosion protection of steel by PANI coatings has also been studied, and a number of operating mechanisms were reported such as anodic protection, barrier protection, corrosion inhibitors, shift of electrochemical interface, etc [21, 22].

In recent decades, several studies have been carried out to enhance PANI-metal oxide hybrid nanocomposites materials [23]. The electrical property of PANI is an important factor which could be modified by the addition of inorganic fillers such as metal oxide nanostructures with dimensions in the nano-scale. It was also reported that the electrical conductivity of PANI can be influenced by dopant ions used in the synthesis of PANI polymer [24-26]. Unfortunately, thin layer of conducting polymers can give protection of the substrate only for a short period.

Several reports have been mentioned that organic-inorganic hybrid nanocomposite coatings can increase the corrosion resistance of metallic substrates such as aluminum [27], iron [28, 29]², copper [30-33] and magnesium [34]. It is also reported that coatings containing metal oxide nanoparticles such as Na⁺-MMT [35], TiO₂ [36, 37], ZnO [38] and Fe₂O₃ [39]

have better corrosion protection abilities due to uniform distribution of PANI and possibility of formation of uniform passive layers on the surface of the metallic substrate. Thus, PANI-metal oxide nanocomposite materials are the potential candidates to add into organic coatings as advanced anti-corrosion additives.

Magnetic nano materials have been the subject of increasing interest because of their physical properties and technological applications. The iron oxide (Fe₂O₃) has the important magnetic properties. From the viewpoint of the basic research, Fe₂O₃ is a convenient compound for the general study of polymorphism and the magnetic and structural phase transitions of nanoparticles. The existence of amorphous Fe₂O₃ and its three polymorphs (α , β , γ) is well established. The most frequent polymorphs structure “ α ” (hematite) having a rhombohedral-hexagonal, prototype corundum structures, and cubic spinel structure “ γ ” (maghemite) have been found in nature [40].

The main aim of the present study is to electropolymerize of PANI and PANI-Fe₂O₃ nanocomposite on AA5052 electrode from an aqueous oxalic acid solution via the galvanostatic method by optimizing the direct electrodeposition conditions. The aqueous electrochemical process is an environmental friendly and efficient technique used to process conducting polymer coatings. It is widely preferred because of its simplicity and it also can be used as a one-step method to form coatings on metal substrates. It allows efficient control of the chemical and physical properties of the coatings, and it can also be easily adapted to large-scale production. Aluminum alloy 5052 has nominally 2.5% magnesium & 0.25% chromium. It has good workability, medium static strength, high fatigue strength, good weld ability, and very good corrosion resistance, especially in marine atmospheres. It also has the low density and excellent thermal conductivity

common to all aluminum alloys. It is commonly used in sheet, plate and tube form.

In this work, strongly and adherent PANI and PANI-Fe₂O₃ nanocomposite coatings on AA5052 were electrochemically synthesized by using the direct electrochemical galvanostatic method. The coatings were then characterized by FT-IR, UV-Vis, SEM-EDX and SEM. The anti-corrosion performance of the coated samples with PANI and PANI-Fe₂O₃ nanocomposite were then evaluated by of open-circuit potential (OCP), Tafel polarization and EIS techniques in 3.5% NaCl.

2. Material and methods

α -Fe₂O₃ was purchased from US Research Nanomaterials (size 20-50 nm). All other chemicals were purchased from Merck. Aniline was freshly distilled and stored in the dark. All solutions were freshly prepared from analytical grade chemical reagents using doubly distilled water. For each run, a freshly prepared solution and a cleaned set of electrodes were used, and all experiments were carried out at room temperature.

Electrochemical experiments and corrosion tests were carried out using a μ -AUTOLAB potentiostat/galvanostat model μ III AUTO71174 connected to a Pentium IV personal computer through a USB electrochemical interface. Pretreated AA5052 was used as working electrode in the conventional three-electrode cell. The auxiliary electrode was a large Pt sheet and an Ag/AgCl (in 3 M KCl) electrode was used as a reference electrode.

The working electrode was prepared from an AA5052 sheet with the chemical composition (wt. %) of: Si (0.25), Fe (0.40), Cu (0.10), Mn (0.10), Mg (2.40), Zn (0.10), Cr (0.25) and Al (96.40). The metal sheet was cut into rectangular samples of 1 cm² area soldered with Al-wire for an electrical connection. The metal sheet then mounted onto the epoxy resin to offer only one active flat surface exposed to the

corrosive environment. Before each experiment, the working electrode was abraded with a sequence of emery papers of different grades (200- 2500) and the polished electrode was degreased with acetone and then immersed in 5% NaOH solution for 2 minutes for activating the surface. After this stage, the electrode cleaned with detergent powder to remove the black colored smudge formed over the surface and washed thoroughly with running water and dipped in a concentrated H₃PO₄ solution for 30 s. The electrode was then washed with distilled water and used for electropolymerization.

Electropolymerization was carried out by the galvanostatic method with 20 ml solution included of the 0.5 M oxalic acid and 0.1 M aniline. As a typical procedure for the preparation of the PANI- Fe₂O₃ nanocomposite coatings, a mixture of 0.5 M oxalic acid and 0.1 M aniline monomer with 1 wt% of dispersed Fe₂O₃ nanoparticles was prepared. The obtained dispersion was put in an ultrasonic instrument for 30 min in order to increase its uniformity. In this regard, six current densities were applied, and the corresponding potential transients were recorded for a period of 1800 sec.

The FT-IR spectrum of electrosynthesized PANI over AA5052 was obtained using a Shimadzu Varian 4300 spectrophotometer in KBr pellets. The electrosynthesized PANI was dissolved in pure N-methylpyrrolidone (NMP) and UV-Vis spectrum of this polymer solution was recorded on a Perkin Elmer Lambda2S UV-Vis spectrometer. The morphology of the electropolymerized PANI-Fe₂O₃ nanocomposite coatings on AA5052 was analyzed using a SERON model AIS-2100 scanning electron microscope instrument operating at 10 kV equipped with an energy dispersive X-ray (SEM-EDX) spectroscopy. The samples were mounted on a double-sided adhesive carbon disc and sputter coated with a thin layer of gold to prevent sample charging problems.

The AA5052 samples with electrosynthesized PANI and PANI-Fe₂O₃ nanocomposite coatings were evaluated for their corrosion protection performance in 3.5% NaCl by Tafel polarization and electrochemical impedance spectroscopy (EIS). The working electrode was first immersed in the test solution for 1800 s to establish a steady state open-circuit potential (OCP).

In the case of Tafel polarization, the potential was scanned at -200 to +200 mV versus OCP at a scan rate of 0.001 mV s⁻¹. From the anodic and cathodic polarization curves, the Tafel regions were identified and extrapolated to the corrosion potential (E_{corr}) to get the corrosion current (I_{corr}) using the NOVA 1.6 software. In the case of electrochemical impedance spectroscopy, a.c. signals of 10 mV amplitude and various frequencies from 100 kHz to 0.01 Hz at open circuit potentials were impressed to the coated AA5052 in the electrode surface (1 cm²). A Pentium IV powered computer and NOVA 1.6 software was applied for analyzing impedance data.

3. Results and discussion

3.1. Electropolymerization

The experiments were performed under galvanostatic conditions. The E-t transient curves were obtained during the formation of PANI and PANI-Fe₂O₃ nanocomposite coatings on AA5052 for six different applied current densities 2.5, 5, 10, 15, 20 and 25 mA cm⁻² (Fig.1 a and b). Coatings of homogeneous appearance were obtained at all applied current densities.

The time to reach the maximum potential value is different for the applied current densities that it is nominated as induction time. Also, less induction time is needed for synthesized PANI-Fe₂O₃ nanocomposite coating comparing to PANI.

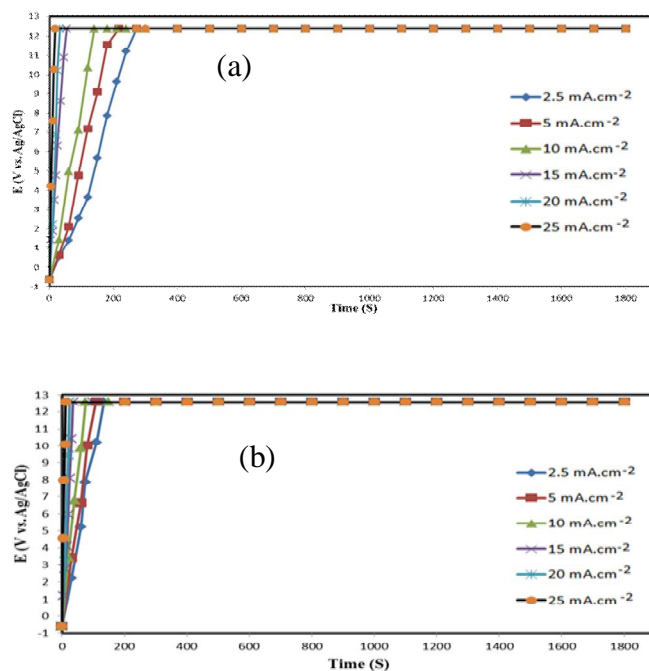


Fig. 1. E-t curve under galvanostatic polymerization conditions in 0.5 l (a) acetic acid solution containing (a) 0.1 M aniline and (b) 0.1 M aniline and 1 wt% dispersed Fe₂O₃ nanoparticles for AA5052 electrode at various current densities (mA cm⁻²).

The PANI and PANI-Fe₂O₃ nanocomposite coatings synthesized by a current density of 25 mA cm⁻² is an adhesive and uniform and they are not destroyed since washed with ethanol and water. The galvanostatic procedure gave rise to the deposition of a green coating, characteristic of PANI and PANI-Fe₂O₃ nanocomposite in the emeraldine oxidation state on the surface of AA5052.

3.2. Characterization of PANI-Fe₂O₃ nanocomposite films

Fig. 2 shows the UV-visible spectrum in pure NMP solvent for PANI and PANI-Fe₂O₃ nanocomposite coatings obtained under galvanostatic conditions on the surface of AA 5052. Fig. 2 shows a broad absorption band at 300 and 620 nm. The absorption band at 300 nm can be attributed to the π^* transition in the benzeneoid ring of the polymer. The peak at

620 nm can be attributed to inter molecular transition between the benzenoid and quinoid moieties in the polymer [41]. The presence of peak suggests that a certain amount of conjugation. From Fig 2, it can see that there is almost no absorption in the wavelength range from 400 to 800 nm, indicating that this nanocomposite is transparent in visible light region. Compared with the UV-vis absorption spectra of PANI, the peak at 620 nm is red shifting and flattening, shows the interaction between the Fe_2O_3 nanoparticles and PANI [42].

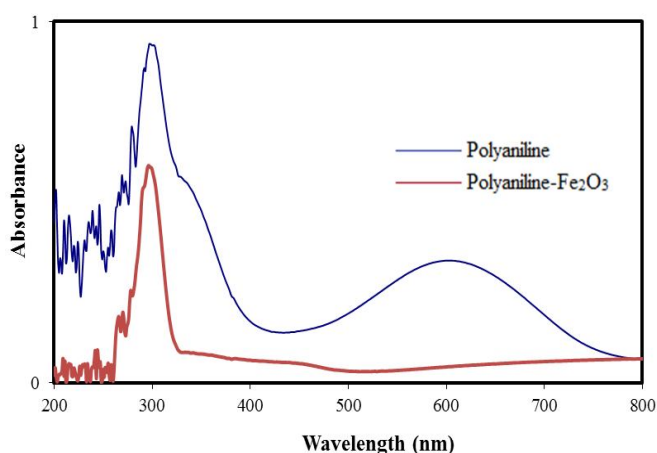


Fig. 2. UV-Vis spectrum recorded for the electrosynthesized pure PANI and PANI- Fe_2O_3 nanocomposite on the AA5052 electrode.

The typical FT-IR absorbance spectrum for Fe_2O_3 , PANI, and PANI- Fe_2O_3 nanocomposite are shown in Fig. 3. In the spectrum of the PANI- Fe_2O_3 nanocomposite, characteristic absorbance bands of PANI and Fe_2O_3 nanoparticles occurred at the following locations: the peak at 3500 cm^{-1} is due to the N-H stretching vibration of secondary amine, the aromatic C-H stretching vibration at about 2200 cm^{-1} , C-N stretching vibration at 1350 cm^{-1} and the in-plane C-H bending at about 1200 cm^{-1} reveal the characteristic bands of PANI. The bands at approximately 1550 and 1450 cm^{-1} are due to the benzenoid and quinoid ring units, respectively. It was found the PANI coating formed by galvanostatic

conditions contained both benzenoid and quinoid moieties. The peak 750 cm^{-1} is assigned to out of plane C-H deformation of aromatic rings. The FTIR spectrum shown characteristic absorption at 1700 and 1200 cm^{-1} correspond to the Fe-O vibrations in Fe_2O_3 nanoparticles [39, 40, 43]. The prominent peaks of PANI and Fe-O vibration of Fe_2O_3 , however C=N, C=C, and C-N absorption bands of PANI- Fe_2O_3 were slightly shifted to lower wavenumbers when compared with that of PANI [43]. This shift may be due to some electronic interaction between PANI chains and surface of Fe_2O_3 that Fig 4 shows the structure of PANI- Fe_2O_3 nanocomposite, therefore all confirm the presence of Fe_2O_3 nanoparticles in the PANI- Fe_2O_3 nanocomposite coatings. Therefore, the FT-IR technique confirms the incorporation of Fe_2O_3 nanoparticles in PANI matrix that was formed using an electropolymerization method for nanocomposite preparation [40].

The EDX data of PANI- Fe_2O_3 nanocomposite is shown in Fig. 5. Nano- Fe_2O_3 shows peaks at 0.3, 0.6 and 6.5 keV are related to O and Fe, respectively. These results confirm that Fe and O exist in the nanocomposite structure on the aluminum alloy surface and a peak toward 1.5 keV is related to aluminum of the substrate [44].

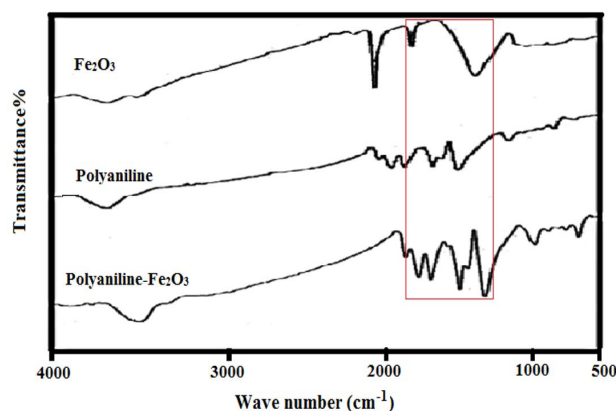


Fig. 3. FT-IR spectrum (a) Fe_2O_3 nanoparticles (b) PANI and (c) the PANI- Fe_2O_3 nanocomposite.

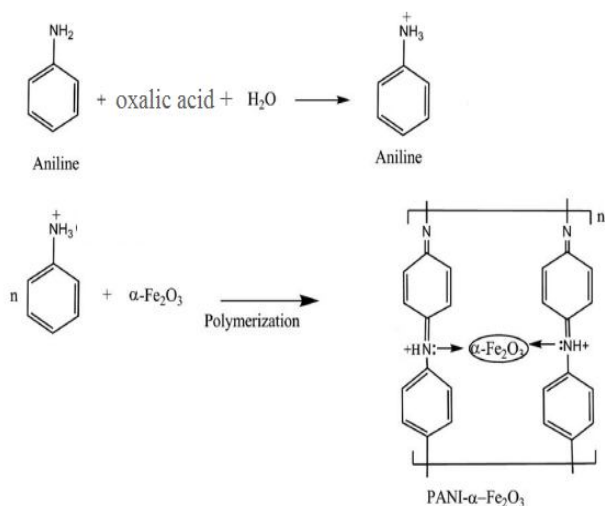


Fig. 4. The structure of PANI -Fe $_2$ O $_3$

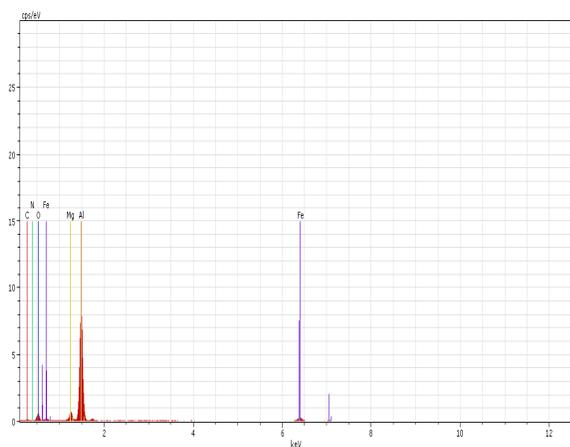


Fig. 5. EDX pattern of the electrosynthesized PANI-Fe $_2$ O $_3$ nanocomposite coated AA5052 for 25 mA cm $^{-2}$.

3.3. Corrosion protection evaluation of the coatings

The corrosion protection performance of PANI-Fe $_2$ O $_3$ nanocomposite and PANI coatings synthesized under galvanostatic conditions was examined in an aqueous 3.5 wt% NaCl solution using open-circuit potential (OCP), Tafel polarization and electrochemical impedance spectroscopy (EIS) studies.

Open-circuit potential uncoated and coated with PANI and PANI-Fe $_2$ O $_3$ nanocomposite of AA5052

electrodes with different current density were measured against time in 3.5% NaCl solution. Fig. 6 shows the variations of OCP with time for AA5052 coated electrode. Initially, all samples were immersed in 3.5% NaCl and their potentials were measured. Periodic measurements of OCP were carried out on the coating systems and all results were documented which are given in Fig. 6. It is obvious that OCP are gradually shifted to the active potentials (cathodic direction) for PANI -Fe $_2$ O $_3$ coatings with time after up to 2 h. In the case of PANI -Fe $_2$ O $_3$ coating, the first potential was -0.731 V. With the passage of time, the potential moved toward active regions and reached a maximum potential value of -0.760 V after 1800 s immersion in 3.5% NaCl solution. In the other words, in the beginning, the potential values were shifted toward cathodic direction after 1800 s immersion in 3.5% NaCl solution.

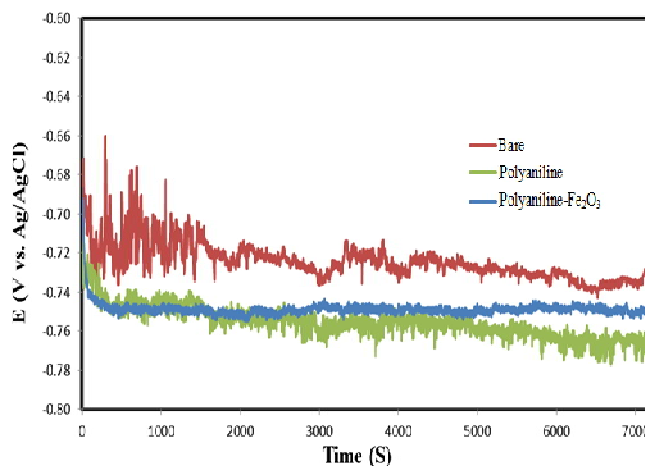


Fig. 6. OCP plots PANI and PANI-Fe $_2$ O $_3$ of coated AA5052 during 2 h immersion in 3.5% NaCl.

In fact, reduction in potential values showed that diffusion of electrolyte and corrosive ions took place through defects and pinholes which existed in the coatings [45]. Similar results for PANI containing coating were reported by Sathiyarayanan et al.[46] and this phenomenon can be attributed to ability of

PANI coatings in the formation of the passive layer on AA5052 substrate.

The Tafel polarization curves recorded in 3.5% NaCl solution for an uncoated AA5052, PANI and PANI - Fe₂O₃ nanocomposite coated AA5052 are shown in Fig. 7 a and b. The values of the E_{corr}, I_{corr}, polarization resistance (R_{pol}) and corrosion rate (C_R) obtained from these curves are given in Table 1. It was clear that the current values of the coated sample are lower than that of the bare sample and corrosion potential of the coated sample is shifted to cathodic direction. From the measured corrosion current density values, the protection efficiency (PE) was obtained from the following equation [47]:

$$PE\% = [(I_{corr} - I_{corr(c)}) / I_{corr}] \times 100 \quad (1)$$

where I_{corr} and I_{corr(c)} are the corrosion current density values in the absence and presence of polymer coating respectively.

The decrease in the I_{corr} was observed 885.3 μA cm⁻² for uncoated AA5052 to 170.1 and 23.3 μA cm⁻² for PANI and PANI - Fe₂O₃ nanocomposite coatings, respectively. The C_R of PANI and PANI - Fe₂O₃ nanocomposite coated AA5052 are found to be 4.7×10⁻⁵ and 7.1×10⁻⁶ mm year⁻¹, respectively, which are about 20 and 140 times lower than that observed for uncoated AA5052 (1.0×10⁻³ mm year⁻¹). This result was pointed out the protective property of the coating against the corrosive medium.

The polarization resistance (R_{pol}) is an important parameter, that ability of a coating in the prevention of electron exchange in a corrosive environment. As it can be seen in Table 1, R_{pol} increases from 3.4×10² Ω cm² for uncoated AA5052 to 3.7×10⁵ and 4.5×10⁶ Ω cm² for PANI and PANI - Fe₂O₃ nanocomposite coated AA5052 under optimal condition. These results show that the coating of PANI - Fe₂O₃ nanocomposite has high polarization resistance.

It can be seen that the corrosion current of the PANI - Fe₂O₃ nanocomposite coated was lower than and PE% is higher than PANI coated AA5052. Therefore, it was found that the incorporation of Fe₂O₃ nanoparticles in the matrix coatings promotes the anti-corrosive efficiency of the PANI - Fe₂O₃ nanocomposite coating on AA5052. However, the enhanced corrosion protection by the PANI - Fe₂O₃ nanocomposite over the protection by the PANI might result from the nano layers of the Fe₂O₃ dispersed in the matrix coatings as filler that increase the tortuosity of the diffusion pathway of corrosive agents such as oxygen gas, hydrogen and chloride ions [48].

The coating porosity is one of the important parameters, which strongly governs the anticorrosive behavior of the coatings. Therefore, measurement of the coating porosity is essential in order to estimate the overall corrosion protection of the coated substrate. In this work, the porosity in PANI and PANI - Fe₂O₃ nanocomposite coatings on AA5052 substrates was determined from polarization resistance measurements. The porosity in polymer coating was calculated using the relation [49]:

$$P = (R_{pol(uc)} / R_{pol(c)}) \times 10^{-((\Delta E) / b_a)} \quad (2)$$

where P is the total porosity, R_{pol(uc)} the polarization resistance of the bare AA5052, R_{pol(c)} the measured polarization resistance of coated AA5052, ΔE_{corr} the difference between corrosion potentials and b_a (b_a= 0.16 V dec⁻¹) the anodic Tafel slope for bare AA5052 substrate. The porosity in PANI and PANI - Fe₂O₃ nanocomposite coatings (25 mA cm⁻²) was found to be 0.01 and 0.002, respectively. As it can be seen, the porosity was decreased in the presence of Fe₂O₃.

Therefore, from the obtained results, it can be concluded that in much higher current densities the PANI and PANI - Fe₂O₃ nanocomposite coated on AA5052 have low porosity cause decreasing of the corrosion current and also is increasing of PE%.

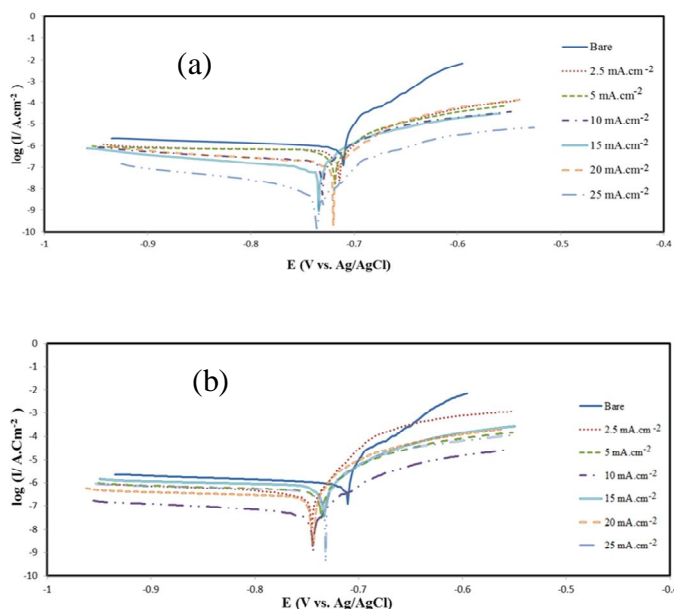


Fig. 7. Polarization behavior of electropolymerized (a) PANI, (b) PANI-Fe₂O₃ nanocomposite-coated on AA5052 at various current densities (mA cm⁻²) in 3.5% NaCl.

For further study corrosion protection performance of prepared coatings, EIS technique was used to determine the protective properties of the coating by measuring different parameters including coating resistance (R_{por}), double layer capacitance (C_{dl}), solution resistance (R_s), charge transfer resistance (R_{ct}) and coating capacitance (C_c) of the prepared coatings. The equivalent circuits fitted with the Nyquist plots are shown in Fig. 8 a & b.

In the presence of defects in the coating, water molecules and ions can easily transfer through the film. R_{ct} can be attributed to the electrical resistance owing to the ionic transfer through the coating pores and it normally decreases with exposure time in corrosive media due to the penetration of electrolytes through the coating pores and defects.

The impedance parameter values of the best fit to the experimental data using the circuit that is shown in Fig. 9 [50, 51] as a function of applied current density for the galvanostatic deposition of the decreases PANI-Fe₂O₃ nanocomposite and PANI on AA5052 are shown in Table 2.

From the measured charge transfer resistance values, the PE% of the coating was obtained from the following equation [52]:

$$\text{PE} = \left[\frac{R_{\text{ct}(c)} - R_{\text{ct}}}{R_{\text{ct}(c)}} \right] \times 100 \quad (3)$$

where $R_{\text{ct}(c)}$ and R_{ct} are the charge transfer resistance values in the presence and absence of the polymer coating, respectively.

The R_{ct} values are approximately 14.1 and 25.2 kΩcm² for PANI and PANI-Fe₂O₃ nanocomposite coated AA5052 which are about 5 and 9 times higher than the uncoated AA5052, respectively. The higher value of the R_{ct} is attributed to the effective barrier behavior of the PANI-Fe₂O₃ nanocomposite coating. The lower values of C_c and C_{dl} for the PANI-Fe₂O₃ nanocomposite coated AA5052 provide further support for the protection of AA5052 by the PANI-Fe₂O₃ nanocomposite coating. Thus, the higher values of R_{ct} and R_{por} and lower values of C_c and C_{dl} indicate the corrosion performance of the PANI-Fe₂O₃ nanocomposite coating.⁴⁸

The changes of the impedance spectra are due to increases of R_{por} and R_{ct} with d increases. With increasing coating thickness the changes of the spectra in the low-frequency region become less pronounced. At high frequencies the data are dominated by electrolyte resistance while at very low frequencies the impedance is dominated by the oxide film resistance. At medium frequencies the capacitive behavior of the system is evident, determined by the dielectric properties of the naturally formed oxide film.

The values of the polarization resistance can be determined using the equivalent circuit model by subtracting the pore resistance and solution resistance from total coating resistance. As it can be seen, the decline of impedance values in the lower frequency region can be interpreted as the delaminating of the coating, although the film was not physically detached

from the substrate metal surface in the microscopic sense [53-55].

On the other hand, these results show that the barrier properties of the coating on the AA5052 surface increased. The PE% calculated from EIS data is found to be 80.5% and 89.1% for PANI and PANI-Fe₂O₃ nanocomposite-coated AA5052, respectively, which are in agreement with the potentiodynamic polarization results. It can be seen that the incorporation of Fe₂O₃ nanoparticles into the PANI matrix exhibited better charge transfer resistances than PANI-coated AA5052 electrodes.

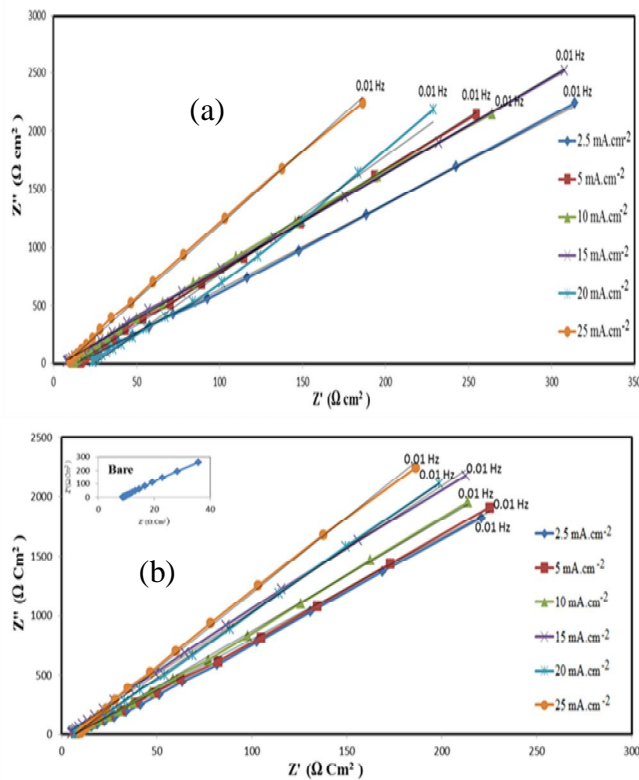


Fig. 8. Nyquist impedance plots for uncoated AA5052, (a) PANI and (b) PANI- Fe₂O₃ coated AA5052 synthesized under galvanostatic conditions at various current densities (mA cm⁻²).

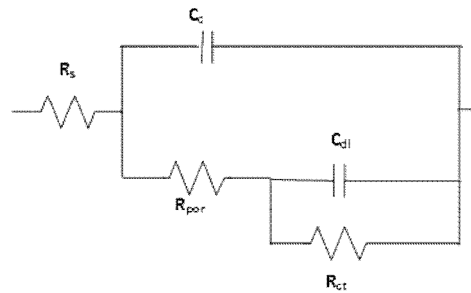


Fig. 9. Equivalent circuit model

One of the important parameters for synthesis of the polymer coatings on the metal surface is calculating coating thickness which is an important feature for industrial applications. EIS data can be used for measurement of the thickness of PANI coatings. The PANI and PANI-Fe₂O₃ nanocomposite coating thickness on the surface of AA5052 by using of C_c can be achieved according to the following equation [56]:

$$C_c = \epsilon_0 \epsilon A / d \tag{4}$$

where ϵ is the dielectric constant of the coating layer, ϵ_0 is the vacuum permittivity, A is the electrode area and d is the thickness of the protective layer. As can be seen in Table 2 with increasing of applied current density, thickness increased and coating capacitance reduced. According to Table 2, it can be concluded that the protection efficiency increased when coating thickness increased. On the other hand, these results show that the barrier properties of the coating on the AA5052 surface increased.

Table 1. Electrochemical parameters of electropolymerized PANI and PANI-Fe₂O₃ nanocomposite on AA5052 in aqueous 3.5% NaCl solution under the galvanostatic conditions at different current densities for 1800 s

Coatings	Sample	E _{corr} (V vs. Ag/AgCl)	I _{corr} (μA cm ⁻²)	R _{pot} (Ω cm ²)	C _R (mm year ⁻¹)	PE%	Por%
PANI	Bare	-0.710	885.3	3.4×10 ²	1.0×10 ⁻³	-	-
	2.5 mA cm ⁻²	-0.714	280.0	1.8×10 ⁴	5.2×10 ⁻³	68.3	0.20
	5.0 mA cm ⁻²	-0.719	249.5	2.2×10 ⁴	4.0×10 ⁻³	71.8	0.17
	10.0 mA cm ⁻²	-0.728	218.3	6.4×10 ⁴	7.4×10 ⁻⁴	75.3	0.07
	15.0 mA cm ⁻²	-0.741	201.3	8.9×10 ⁴	1.5×10 ⁻⁴	77.2	0.06
	20.0 mA cm ⁻²	-0.721	189.1	2.1×10 ⁵	4.0×10 ⁻⁴	78.6	0.02
PANI-Fe ₂ O ₃	25.0 mA cm ⁻²	-0.795	170.1	3.7×10 ⁵	4.7×10 ⁻⁵	80.7	0.01
	2.5 mA cm ⁻²	-0.745	184.7	5.2×10 ⁴	3.7×10 ⁻³	79.1	0.040
	5.0 mA cm ⁻²	-0.735	156.4	7.5×10 ⁴	5.5×10 ⁻³	82.3	0.031
	10.0 mA cm ⁻²	-0.744	73.9	2.3×10 ⁵	3.2×10 ⁻⁴	91.6	0.009
	15.0 mA cm ⁻²	-0.733	46.7	4.6×10 ⁵	1.8×10 ⁻⁴	94.7	0.005
	20.0 mA cm ⁻²	-0.743	29.2	7.1×10 ⁵	4.6×10 ⁻⁵	96.7	0.003
	25.0 mA cm ⁻²	-0.731	23.3	4.5×10 ⁶	7.1×10 ⁻⁶	97.3	0.002

3.3. Morphological investigation of coatings by SEM method

The surface morphologies of the coatings were characterized by scanning electron microscopy (SEM). SEM micrographs obtained from AA5052 surface specimens immersion in 3.5% NaCl for 5 days. The SEM images of abraded AA5052 (a), pre-treated AA5052 after corrosion (b), PANI coating after corrosion (c), and PANI-Fe₂O₃ nanocomposite coating grown by an applied current density of 25mA cm⁻² after corrosion (d) are shown in Fig. 10. Image (b) shows that numerous large pits and inequalities were formed after corrosion, which reveals severe damage on the surface because of metal dissolution. Image (c) shows that the PANI coating was electrodeposited on the surface and

Table 2. Impedance parameter values of the electrosynthesized PANI and PANI-Fe₂O₃ nanocomposite extracted from the fit to the equivalent circuit for the impedance spectra recorded in aqueous 3.5% NaCl solution.

Coatings	Sample	R _s (Ω cm ²)	C _c (F cm ²)	R _{por} (Ω cm ²)	R _{ct} (kΩ cm ²)	C _{dl} (F cm ²)	d ¹ (μm)	PE%
PANI	Bare	8.8	4.9×10 ⁻⁸	77.5	2.75	1.5×10 ³	-	-
	2.5 mA cm ⁻²	9.5	6.2×10 ⁻⁷	421	7.4	5.9×10 ⁷	1.2	62.8
	5.0 mA cm ⁻²	14.1	5.7×10 ⁻⁷	613	8.5	2.2×10 ⁷	1.4	67.6
	10.0 mA cm ⁻²	9.5	4.0×10 ⁻⁷	989	9.9	1.9×10 ⁷	2.0	72.2
	15.0 mA cm ⁻²	16.1	3.6×10 ⁻⁷	1010	11.2	1.7×10 ⁷	2.2	75.4
	20.0 mA cm ⁻²	23.2	3.0×10 ⁻⁷	820	13.4	1.5×10 ⁷	2.6	79.5
PANI-Fe ₂ O ₃	25.0 mA cm ⁻²	9.5	2.2×10 ⁻⁷	988	14.1	1.2×10 ⁷	3.5	80.5
	2.5 mA cm ⁻²	11	5.2×10 ⁻⁷	526	13.8	2.6×10 ⁷	1.5	80.0
	5.0 mA cm ⁻²	10.6	4.0×10 ⁻⁷	687	15.2	1.8×10 ⁷	2.0	81.9
	10.0 mA cm ⁻²	13.8	3.0×10 ⁻⁷	1430	17.0	1.5×10 ⁷	2.6	83.8
	15.0 mA cm ⁻²	12.4	2.0×10 ⁻⁷	1546	18.9	8.7×10 ⁸	4.0	85.4
	20.0 mA cm ⁻²	13.8	1.2×10 ⁻⁷	1589	23.5	6.5×10 ⁸	6.5	88.3
	25.0 mA cm ⁻²	12.4	8.7×10 ⁻⁸	1643	25.2	4.8×10 ⁸	9.0	89.1

*(ε₀=8.85×10⁻¹² F/cm, ε=5.9 F/cm, A=1 cm²)

protected it from the corrosion, and image (d) shows that the PANI-Fe₂O₃ nanocomposite coating protects the AA5052, which does not change dramatically. It clearly reveals that the formed coatings on AA5052 surface are uniform and dense. The quality of the coatings is so that no crack or detachment of the coatings is observed. Thus, morphological studies of all coatings can support attained results such as electrochemical studies as well.

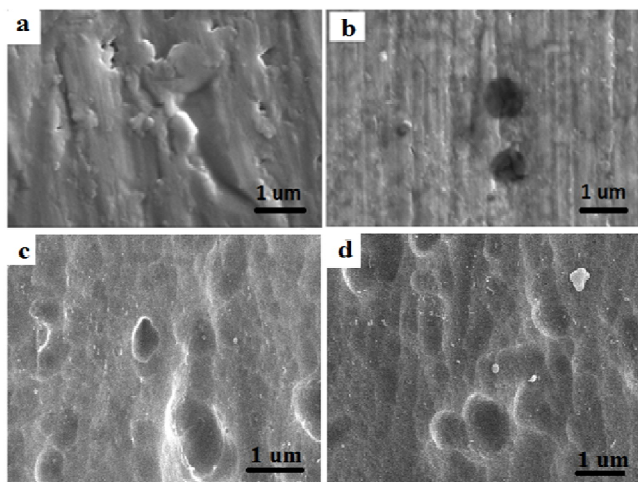


Fig. 10. SEM micrographs of abraded AA5052 (image a) pre-treated AA5052 after corrosion (image b), PANI coating after corrosion (image c) and PANI-Fe₂O₃ nanocomposite coatings grown by an applied current density of 25 mA cm⁻² after corrosion (image d).

4. Conclusions

The PANI and PANI -Fe₂O₃ nanocomposite coatings were successfully direct electrosynthesized on AA5052 substrates from aqueous solutions containing H₂C₂O₄ and aniline monomers with dispersed Fe₂O₃ nanoparticles for nanocomposite. Uniform, compact and adherent coatings can be obtained under galvanostatic condition. Six various current densities of 2.5, 5, 10, 15, 20 and 25 mA cm⁻² were applied to the formation of PANI and PANI -Fe₂O₃ nanocomposite coatings on AA5052. The results showed that the current density of 25 mA cm⁻² for the polymerization stage is the best condition for the synthesis of more compact and strongly adherent PANI and PANI -Fe₂O₃ nanocomposite coatings on AA5052. The PANI and PANI -Fe₂O₃ nanocomposite coatings were characterized by FT-IR, UV-Vis and SEM-EDX and the corrosion protection performance of the electropolymerized coatings were evaluated using Tafel polarization and electrochemical impedance spectroscopy in 3.5% NaCl solution. The coating porosity was estimated by

using the Tafel polarization measurements and it was found that the porosity values are lower for the PANI-Fe₂O₃ nanocomposite coatings as compared to the PANI. The EIS results are in good agreement with the Tafel polarization measurements. This study reveals the PANI-Fe₂O₃ nanocomposite coating has corrosion protection properties and can be considered as a possible coating material to protect AA5052 against corrosion in solution 3.5% NaCl solution. The enhanced corrosion protection effect of the PANI-Fe₂O₃ nanocomposite relative to PANI in the form of coating on metallic surface was attributed to the combination of the electrochemical property of the PANI and the barrier effect of the Fe₂O₃ nanoparticles dispersing in the composite. We believe that the coating helps to stabilize the passive film onto the substrate thus stopping the AA5052 corrosion.

Acknowledgement

The authors are grateful to University of Kashan for supporting this work by Grant No (159194/8).

References

- [1] V. Karpagam, S. Sathiyarayanan, G. Venkatachari, *Curr. Appl. Phys.* 8 (2008) 93-98.
- [2] K. Kamaraj, S. Sathiyarayanan, G. Venkatachari, *Prog. Org. Coat.* 64 (2009) 67-73.
- [3] J. Huang, J. A. Moore, J. H. Acquaye, R. B. Kaner, *Macromolecules.* 38 (2005) 317-321.
- [4] K. M. Cheung, D. Bloor, G. C. Stevens, *Polymer.* 29 (1988) 1709-1717.
- [5] C. A. Ferreira, S. Aeiych, M. Delammer, P. C. Lacaze, *J. Electroanal.Chem.* 284 (1990) 351-369.
- [6] G. Troch Nagels, R. Winand, A. Weymeersch, L. Renard, *J. Appl. Electrochem.* 22 (1992) 756-764.
- [7] F. Beck, R. Michaelis, *J.Coat. Technol.* 64 (1992) 59-67.
- [8] F. Beck, R. Michaelis, F. Schloten, B. Zinger, *Electrochim. Acta.* 39 (1994) 229-234.

- [9] S. Wenchang, J. O. Iroh, *Electrochim. Acta.* 46 (2000) 1-8.
- [10] G. K. Prasad, T. Takei, Y. Yonesaki, N. Kumada, N. Kinomura, *Mater. Lett.* 60 (2006) 3727-3730.
- [11] B. K. Sharma, A. K. Gupta, N. Kharea, S. K. Dhawan, H. C. Gupta, *Synth.Met.* 159 (2009) 391-395.
- [12] J. Deng, C. L. He, Y. Peng, J. Wang, X. Long, P. Li, Chan, A.S.C, *Synth. Met.* 139 (2003) 295-301.
- [13] N. G. Deshpande, Y. G. Gudage, R. Sharma, J. C. Vyas, J. B. Kim, Y. P. Lee, *Sens. Actuators B.* 138 (2009) 76-84.
- [14] W. Jia, E. Segal, D. Kornemandel, Y. Lamhot, M. Narkis, A. Siegmann, *Synth. Met.* 128 (2002) 115-120.
- [15] K. Gurunathan, D. P. Amalnerkar, D. C. Trivedi, *Mater. Lett.* 57 (2003) 1642-1648.
- [16] B. H. Shambharkar, S. S. Umare, *Mater. Sci. Eng. B.* 175 (2010) 120-128.
- [17] W. Xue, K. Fang, H. Qiu, J.Li, W. Mao, *Synth. Met.* 156 (2006) 506-509.
- [18] S. Sathiyarayanan, S. S. Azim, G. Venkatachari, *Prog.Org.Coat.* 59 (2007) 291-296.
- [19] M. G. Hosseini, M. Jafari, R. Najjar, *Surf.Coat. Technol.* 206 (2011) 280-286.
- [20] E. Akbarinezhad, M. Ebrahimi, H. R. Faridi, *Prog.Org.Coat.* 64 (2009) 361-364.
- [21] G. Mengoli, M. T. Munari, P. Bianco, M. j. Musiani, *Appl. Polym. Sci.* 26 (1981) 4247-4257.
- [22] D. W. J. DeBerry, *Electrochem. Soc.* 132 (1985) 1022-1026.
- [23] P. A. Sorensen, S. Kiil, K. Dam-Johansen, C. E. Weinell, *J Coat Technol. Res.* 6 (2009) 135-176.
- [24] M. M. Ayad, E. A. Zaki, *Eur. Polym. J.* 44 (2008) 3741-3747.
- [25] S. F. Chung, T. C. Wen, A. Gopalan, *Mater. Sci. Eng. B.* 116 (2005) 125-130.
- [26] Y. Long, Z. Chen, N. Wang, J. Li, M. Wan, *Physica B.* 344 (2004) 82-87.
- [27] M. G. Hosseini, M. Jafari, R. Najjar, *Surf. Coat. Technol.* 206 (2011) 280-286.
- [28] A. J. Dominis, G. M.Spinks, G. G.Wallace, *Prog.Org.Coat.* 48 (2003) 43-49.
- [29] A. Olad, R. Nosrati, *Prog. Org. Coat.* 68 (2012) 319-322.
- [30] T. Tüken, B.Yazıcı, M. Erbil, *Prog.Org. Coat.* 51 (2004) 152-160.
- [31] M. Sharifirad, A. Omrani, A. A Rostami, M. Khoshroo, *J. Electroanal. Chem.* 645 (2010) 149-158.
- [32] M. Bazzaoui, J. I. Martins, E. A. Bazzaoui, T. C. Reis, L. Martins, *J. Appl. Electrochem.* 34 (2004) 815-822.
- [33] M. I. Redondo, C. B. Breslin, *Corr. Sci.* 49 (2007) 1765-1776.
- [34] M. C. Turhan, M. Weiser, H. Jha, S. Virtanen, *Electrochim. Acta.* 56 (2011) 5347-5354
- [35] M. Shabani-Nooshabadi, S. M. Ghoreishi, M. Behpour, *Corrs. Sci.* 53 (2011) 3035-3042.
- [36] M. D. Lenz, C. A. Ferreira, M. Delamar, *Synth. Met.* 126 (2002) 179-182.
- [37] S. Abaci, B. Nessark, *J.Coat. Technol.Res.* 12 (2015) 107-120.
- [38] B. Ramezanzadeh, M. M.Attar, *Prog. Org. Coat.* 71 (2011) 314-328.
- [39] M. J. Palimi, M.Rostami, M. Mahdavian, B. Ramezanzadeh, *J. Coat. Technol. Res.* 12 (2015) 277-292.
- [40] S. S. Umare, B. H. Shambharkar, *J. Appl. Poly. Sci.* 127 (2013) 3349-3355.
- [41] A. Yagan, N. O. Pekmez, A. Yildiz, *Electrochim. Acta.* 51 (2006) 2949- 2955.
- [42] Q. L. Yang, J. Zhai, L. Feng,, Y. L. Song, M. X. Wan, L. Jiang, W. G. Xu, Q. S. Li, *synth Metal.* 135 (2003) 819-820.
- [43] M. S. C. Kumar, V. Selvam, M. Vadivel, *Eng. Sci. Adv. Technol.* 2 (2012) 1258-1263.
- [44] Sh. W. Cao, J. Fang, M. M. Shahjamali, Zh. Wang, Zh.Yin, Y. Yang, F. Y. C.Boey, J. Barber, S.

- Ch. Joachim, C. Xue, *Cryst. Eng. Comm.* 14 (2012) 7229-7235.
- [45] S. Sathiyarayanan, S. S. Azim, G. Venkatachari, *Synth. Met.* 157 (2007) 205–213.
- [46] S. Sathiyarayanan, S. S. Azim, G. Venkatachari, *Electrochim. Acta.* 53 (2008) 2087-2094.
- [47] S. Akpolat, S. Bilgic, *Protec. Metal. Physi. Chem. Surfac.* 50 (2014) 266-272.
- [48] M. Shabani-Nooshabadi, S. M. Ghoreishi, M. Behpour, *Electrochim. Acta.* 54 (2009) 6989- 6995.
- [49] S. Chaudhari, S. R. Sainkar, P. P. Patil, *J. Phys. D: Appl. Phys.* 40 (2007) 520- 533.
- [50] N. Jadhar, M. B. Jensen, V. Gelling, *J. Coat. Technol. Res.* 12 (2015) 259-276.
- [51] A. Mostafaei, F. Nasiripouri, *Progre. Organic. Coat.* 77 (2014) 146-159.
- [52] M. Behpour, S. M. Ghoreishi, N. Mohammadi, N. Soltani, M. Salavati-Niasari, *Corros. Sci.* 52 (2010) 4046- 4057.
- [53] S. Radhakrishnan, N. Sonawane, C. R. Siju, *Prog. Org. Coat.* 64 (2009) 383–386.
- [54] S. Sathiyarayanan, S. SyedAzim, G. Venkatachari, *Electrochim. Acta.* 52 (2007) 2068-2074.
- [55] M. R. Mahmoudian, W. J. Basirun, Y. Alias, *Appl. Surf. Sci.* 257 (2011) 3702-3078.
- [56] F. Mansfeld, *J. Appl. Electrochem.* 25 (1995) 187-202.